Numerical Simulation of Sharkskin Phenomena in Polymer Melts

Nattapong Nithi-Uthai, Ica Manas-Zloczower*

Case Western Reserve University, Department of Macromolecular Science
2100 Adelbert Road, Cleveland, Ohio 44106, USA

*Email: ixm@po.cwru.edu
Fax: x1.216.3368-4202

Received: 20.8.2002, Final version: 18.3.2003

Abstract:
A fluid dynamic analysis package, PolyFlow, based on the finite element method is used to study the sharkskin phenomenon. A stick-slip mechanism is used as the basis for the simulations. This study is aimed at illustrating how fluctuations in the stress at the exit from the die cause similar fluctuations in the extrudate swell ratio, resembling the sharkskin phenomenon. Such fluctuations in the stress at the exit from the die are produced by implementing a stick-slip boundary condition at the die wall, mimicking a mechanism of molecular entanglement/disentanglement at the wall. We use a superposition of stress relaxation/stress growth and a periodic change in extrudate swell governed by the die exit stress level to depict sharkskin. Three relatively monodisperse polybutadienes were used in this study. The simulated sharkskin time period was found to be in good agreement with experimental findings. We found that the simulated pictures of sharkskin are similar for all three molecular weight samples. A comparison between the simulated sharkskin and experimental results show qualitative resemblance. The main problems preventing us from generating more quantitative sharkskin results mainly reside in the model limitations in depicting stress singularity, limitations in mesh design refinement and the constitutive model employed. In spite of these limitations, the qualitative agreement between simulation results and experimental data is good.

Zusammenfassung:
Ein Softwarepaket für Fluiddynamik-Simulationen, das auf der Finite-Elemente-Methode beruht, PolyFlow, wird zur Untersuchung des Schmelzbruchverhaltens herangezogen. Ein Rückgleitmechanismus wird als Grundlage der Simulationen benutzt. Die Untersuchung zielt darauf ab, zu veranschaulichen, wie Fluktuationen in den Spannungen am Düsenausgang analoge Fluktuationen im Strangaufweitungsverhältnis verursachen, die Ähnlichkeit mit dem Schmelzbruchphänomen haben. Solche Spannungsfluktuationen am Düsenausgang werden durch Implementation einer Rückgleit-Randbedingung an der Düsenwand realisiert, welche einen molekularen Ver-/Entschlaufungsmechanismus an der Wand nachahmen. Zur Beschreibung des Schmelzbruchs benutzen wir eine Überlagerung von Spannungsrelaxation/Spannungsanstieg und eine periodische Variation der Strangaufweitung welche durch das Spannungsniveau am Düsenausgang bestimmt wird. Drei relativ monodisperse Polybutadiene wurden im Rahmen dieser Untersuchungen benutzt. Die simulierte Schmelzbruchfrequenz stimmte gut mit experimentellen Befunden überein. Wir sahen, dass die aus den Simulationen des Schmelzbruchs erhaltenen Bilder fuür die drei Proben mit unterschiedlichen Molekulargewichten ähnlich sind. Ein Vergleich des simulierten Schmelzbruchs und experimenteller Befunde zeigt qualitative Ähnlichkeit. Die Hauptprobleme, welche eine mehr quantitative Beschreibung des Schmelzbruchs verhindern, liegen in den Beschränkungen des Modells, Spannungssingularitäten vorherzusagen, Beschränkungen in der Verfeinerung der Gitterauflösung, und im konstitutiven Modell, welches benutzt wurde. Trotz dieser Beschränkungen ist die qualtitative Übereinstimmung von Simulationsergebnissen und experimentellen Daten gut.

Résumé:
Polyflow, un logiciel de calcul de dynamique des fluides basé sur la méthode d'éléments finis, est utilisé pour étudier le phénomène de défaut de peau de requin. Un mécanisme d'ancrage-glissement est utilisé comme point de départ des simulations. Cette étude a pour but d'illustrer comment les fluctuations de contrainte à la sortie de la chambre d'extrusion causent des fluctuations similaires dans le ratio de gonflement de l'extrudat, qui ressemblent au phénomène de peau de requin. De telles fluctuations de la contrainte à la sortie de la chambre d'extrusion sont générées en implémentant une condition d'ancrage-glissement à la paroi de la chambre, qui rend compte d'un mécanisme moléculaire d'enchevêtrement/désenchevêtrement à la paroi. Nous utilisons une superposition de relaxation de contrainte/augmentation de contrainte, ainsi qu'un changement périodique dans le gonflement de l'extrudat gouverné par le niveau de la contrainte en sortie de chambre d'extrusion, afin de décrire le défaut de peau de requin. Trois polybutadiènes, relativement monodisperses, ont été utilisés dans cette étude. La période temporelle du défaut de peau de requin simulé concorde bien avec les données expérimentales. Les images de défaut de peau de requin se révèlent être indépendantes du poids moléculaire des échantillons. Une comparaison entre les peaux de requin simulées et les résultats expérimentaux montre une similarité qualitative. Les principaux problèmes qui nous empêchent de générer des résultats plus quantitatifs résident principalement dans les limitations du modèle à décrire la singularité de la c ontrainte, les limitations dans les détails du dessin du maillage, et le modèle constitutif employé. En dépit de ces limitations, la concordance qualitative entre les résultats des simulations et les données expérimentales est bonne.

Key words: sharkskin, flow instabilities, extrudate swell, numerical simulations, finite element method, stress relaxation/stress growth

DOI: 10.1515/arh-2003-0006

© Appl. Rheol. 13 (2003) 79-86

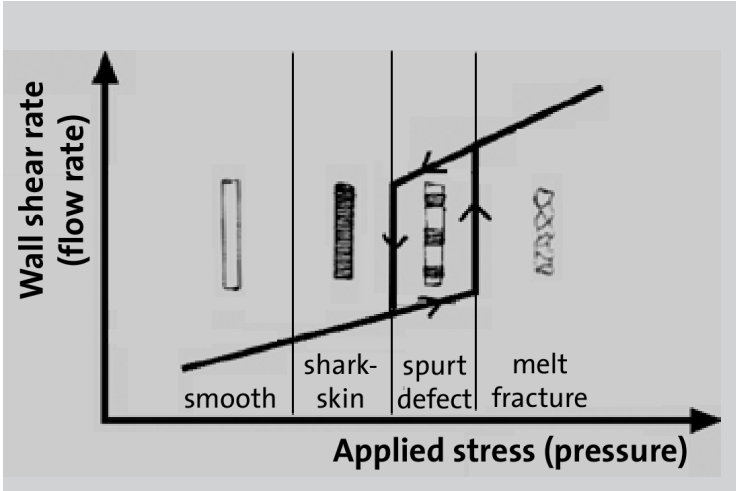

Figure 1: Typical flow curve of polymer melts and general extrudate classifications.

1 INTRODUCTION

Flow instabilities occurring during extrusion of polymeric melts limit the output rates and are detrimental to the quality of the extrudate. In general, upon increasing the output rate, the extrudate surface qualities may change and different extrusion regimes were observed as shown in Figure 1 [1]. Only in a small region denoted as the first regime the extrudate appears smooth and exhibits an acceptable quality for most industrial applications. In all other regimes, flow instabilities occur and distortions of the extrudate can be observed. This classification is by no means universally accepted [2], nevertheless sharkskin is the first extrusion instability observed upon increasing the output rate. Sharkskin is an extrudate distortion with more or less a regular pattern of ridges resulting in an observable opaqueness or roughness. A typical length scale of about 10-100 μm is usually observed (see for instance Figure 4 in reference [3]). This problem not only places strict limits on polymer processing operations but is also raising fundamental challenges stemming from the elastic character of polymeric materials and the complexity of their behavior at fluid/solid interfaces.

As for the mechanism of sharkskin formation, at the present time there is no model able to capture all of the experimental features found in the experiments [4]. The existing models can be classified into two types:

• Heuristic: a narrative describing a plausible scenario based on the observations and some general theoretical considerations

• Analytical: a mathematical formulation of a model problem whose solution explicitly predicts observed features of the phenomenon

However within these boundaries it is common to find models of different type sharing a similar phenomenological point of view. The most popular explanations for sharkskin are constitutive instabilities (analytical type model) and slip at the wall (heuristic type model). In a recent review on extrusion instabilities and wall slip, Denn [5] advances the idea that a rupture mechanism is responsible for sharkskin.

Most simulations of sharkskin fit within analytical models. This study is aimed at illustrating how fluctuations in the stress at the exit from the die cause similar fluctuations in the extrudate swell ratio, resembling the sharkskin phenomenon. Such fluctuations in the stress at the exit from the die are produced by implementing a stick-slip boundary condition at the die wall, mimicking a mechanism of molecular entanglement/disentanglement at the wall [6-9].

2 STICK-SLIP MECHANISM FOR SHARKSKIN

The possible mechanisms of extrusion instabilities have been a subject of debate for a long time. However, researchers seem to agree that sharkskin is an exit effect. In particular, the stress singularity near the die exit causes the sharkskin defect via a mechanism yet to be agreed upon. Wang and co-authors attribute sharkskin formation to time-dependent fluctuations between the stick state and a slip state of the boundary conditions at the polymer/wall interface in the exit region [7]. These authors suggest that the origin of sharkskin dynamics may be related to a molecular instability corresponding to an oscillation of adsorbed chains in the die exit region between coiled and stretched sates [6, 7].

More recently a few studies concentrate on the validity of a no slip boundary condition in polymer melts flows [4, 8]. These studies suggest a minute continual slip of the polymer along the solid surface and the possibility of multiple slip velocities at shear rates close to the point where sharkskin is usually observed. Similar to the mechanism proposed by Wang et al [6,7], Yarin [8] and Graham [4] proposed a mechanism based on entanglement/disentanglement of bulk polymer molecules from the polymer molecules attached to the solid wall. However, Graham's mechanisms depicted more elaborate polymer coil deformation disentanglement.

In the numerical simulations we will use the hydrodynamic stick/slip condition as the basis for sharkskin formation. This stick-slip heuristic mechanism seems mostly consistent with experimental observations and the continuum and molecular theories. Furthermore, it is relying on the existence of a relative motion

Figure 2 (right above): Illustration depicting the spatial variation of stress along the die in both no-slip and slip states: a) as explained by stick-slip mechanism, b) as simulated using slip region.

Figure 3 (right below): Illustration of stick-slip mechanism showing a) oscillation of the true wall shear rate between two values $\dot{\gamma}_o$ and $\dot{\gamma}_s$, b) stress growth/relaxation at the die exit showing periodicity characteristic of sharkskin.

between the polymer near the interface and the interface itself [4].

In extrusion, there are numerous evidences both numerically [10-13] and experimentally [14,15] showing the existence of a stress singularity near the die exit. Figure 2a depicts the stress field along the die land, specifically showing that the die exit stress is higher than the die inland stress. The flow upstream from the die exit is viscometric, i.e. each point in the flow can be specified by a steady shear stress. However as *z* approaches the die exit, the exit stress, σ_{ex}, not only contains a shear component but a significant elongational component due to the boundary discontinuity.

Extensive experimental studies suggest a critical stress, σ_c, above which the polymer will no longer obey the no-slip boundary condition causing a global stick-slip transition [16, 17]. Figure 2 and the existence of a stick-slip transition suggest that a localized stick-slip transition may occur at the die exit. The exit wall stress begins to relax from σ_c to σ_h when such an interfacial transition takes place as illustrated in Fig. 3. Here σ_h denotes the minimum stress level at which the polymer will again stick to the die surface. As illustrated in Fig. 3a, the exit stress σ_{ex} decreases from $\sigma_{ex} = \eta\,\dot{\gamma}_o$ toward $\sigma_s (< \sigma_c) = \eta\,\dot{\gamma}_o$ upon the transition and stops decreasing when reaching σ_h. The no-slip boundary condition becomes valid again, causing the exit stress to grow back toward σ_c. Due to the viscoelastic properties of polymer melts, the stress relaxes and grows in an exponential fashion. This phenomenon persists perpetually, yielding to a periodic oscillation of the true wall shear rate and a stress fluctuation. Rheo-optical studies showed that the stress oscillation at the exit of the die correlates very well with the sharkskin period [14, 15]. Furthermore, differences of stress level on die land via modification of die surface properties lead to different extrudate swell ratios [18]. Intuitively, the stress fluctuation at the die exit ultimately causes an extrudate swell fluctuation, perceived as sharkskin.

3 SIMULATION PROCEDURES

Sharkskin can be viewed as resulting from the superposition of two phenomena, namely a stress relaxation/growth at the die exit, where a

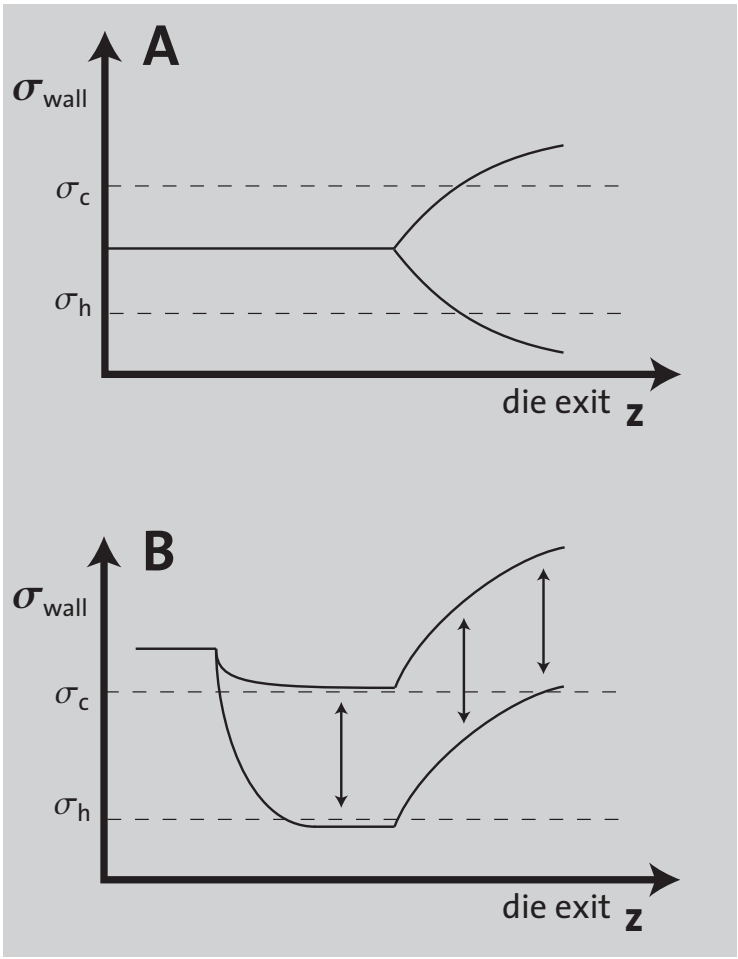

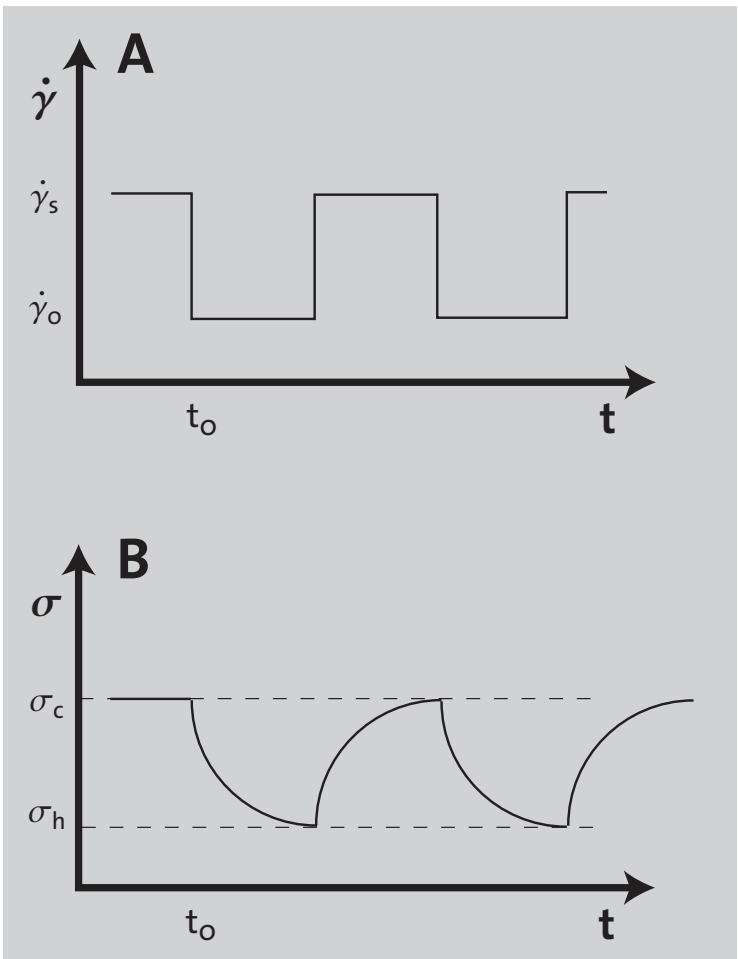

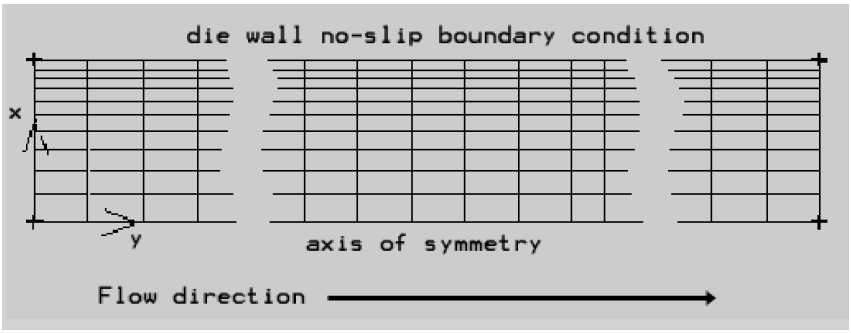

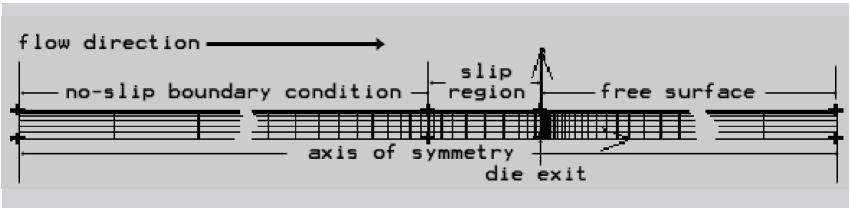

Figure 4 (left above): Mesh design for a) stress relaxation simulation and b) extrudate swell simulation.

periodic stick-slip boundary condition occurs, and consequently, a periodic change in extrudate swell governed by the die exit stress level. We simulate the two phenomena separately. Simulation of stress relaxation/growth will provide information on sharkskin period. This information will be used to simulate extrudate swell at different levels of die exit stress.

Another key information for the simulations are the values of σ_c and σ_h, which set the limits for stress relaxation and stress growth. Barone et al used birefringence to study the stress level at the die exit at which the extrudate exhibits sharkskin [14, 15]. They found that the ratio of σ_h to σ_c is approximately 0.7. We will use this empirical value of 0.7 as the basis of stress fluctuation in our simulation.

A fluid dynamics analysis package PolyFlow based on the finite element method was used in all of our simulations. Simulations were run on SGI Origin 2000 at Ohio Supercomputer Center. The constitutive model used in the simulations is the Giesekus model [19].

Figure 5 (left below): Flow rate used in stress relaxation simulation.

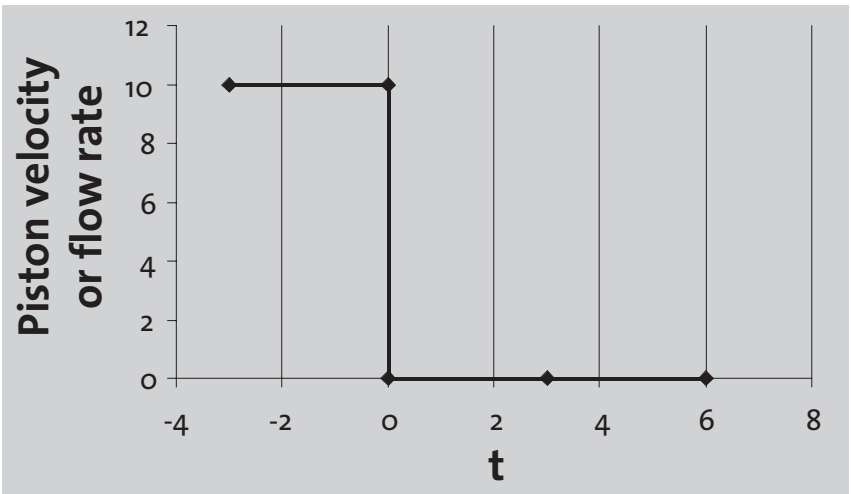

$$\mathbf{T} = \mathbf{T}_1 + \mathbf{T}_2$$
$$\left[\mathbf{T} + \frac{\alpha\lambda}{\eta_1}\mathbf{T}_1\right]\mathbf{T}_1 + \lambda\mathbf{T}_1 = 2\eta_1\mathbf{D}$$
$$\mathbf{T}_2 = 2\eta_2\mathbf{D} \qquad (1)$$

where T is the stress tensor and is a combination of the viscoelastic stress tensor, T_1, and the purely viscous stress tensor, T_2. Parameters α, λ and η are the dimensionless mobility factor, relaxation time and viscosity respectively. D is the rate of strain tensor defined as

$$\mathbf{D} = \frac{1}{2}\left[\nabla v + (\nabla v)^T\right] \qquad (2)$$

Three different relatively monodisperse polybutadienes of molecular weight 50K, 200K and 400K, were used in this study. Rheological data for the samples were obtained using a Rheometrics RMS-800 and were used as an input file in PolyFlow for fitting to a single mode Giesekus model. Details can be found in [21]. All simulations assume an incompressible fluid and isothermal flow, where gravity is neglected.

We carried out time dependent flow simulations to simulate stress relaxation/growth. The continuity equation and the time-dependent momentum equation were solved simultaneously.

$$\nabla \cdot v = 0$$
$$-\nabla P + (\nabla \cdot \mathbf{T}) = \frac{\partial v}{\partial t} + v \cdot \nabla v \qquad (3)$$

Studies showed stress relaxation simulations using Giesekus model to be satisfactory [20]. In this case we used the inertia term, although very small, in order to alleviate numerical instabilities.

Extrudate swell simulations were carried out considering a steady-state condition and assuming equilibrium values for the extrudate swell ratio. More details about equilibrium extrudate swell simulations are discussed elsewhere [21].

4 SIMULATION OF STRESS RELAXATION / STRESS GROWTH

We simulate the stress relaxation upon cessation of flow at the wall of a circular die. The mesh

design for the problem is shown in Fig. 4a. Due to symmetry we can simulate only half of the die. No-slip boundary conditions are applied on the die wall. The steady-state solution for flow through a circular die is used as the starting point in the simulations. At time zero the flow is stopped as illustrated in Fig. 5. This time dependent flow rate is used as boundary condition at the inlet and outlet from the die.

Barone and Wang studied stress relaxation upon the cessation of flow in a slit die through time dependent flow birefringence measurements [14]. These authors used the stress-optical relation and found good correlation between the relaxation portion of the sharkskin cycle and the birefringence relaxation behavior.

We apply a similar rational in our simulations and study the stress relaxation through the time dependent combination of first and second normal stress differences measured at the die wall, i.e. $(N_1 + N_2)_w$, normalized by the maximum total stress at the wall. In the simulations we kept constant the maximum stress at the wall (at 0.31 MPa), such that all three materials experience the same level of deformation. Consequently the flow rate is lower for the higher molecular weights materials.

Results of the stress relaxation simulations are shown in Fig. 6. Assuming that stress growth is similar to stress relaxation, we depict stress growth as the mirror image of stress relaxation. With a value of 0.7 for σ_h/σ_c, we can build the cycle of stress relaxation/stress growth occurring at the die exit during sharkskin formation for the three polybutadienes investigated in this study. The results are presented in Fig. 7.

5 EXTRUDATE SWELL SIMULATIONS

Sharkskin is perceived as an oscillatory (time dependent) extrudate swell. However, one may view it also as a sequence of snapshots of extrudate swell obtained at different levels of stress at the die wall. With this in mind, we wanted to simulate the equilibrium extrudate swell ratio at different conditions (stress levels) at the die exit. However, at the die lip we encounter a stress singularity which is not well defined numerically, and consequently very difficult if not impossible to modify. We address this problem by using a region of slip boundary condition next to the die

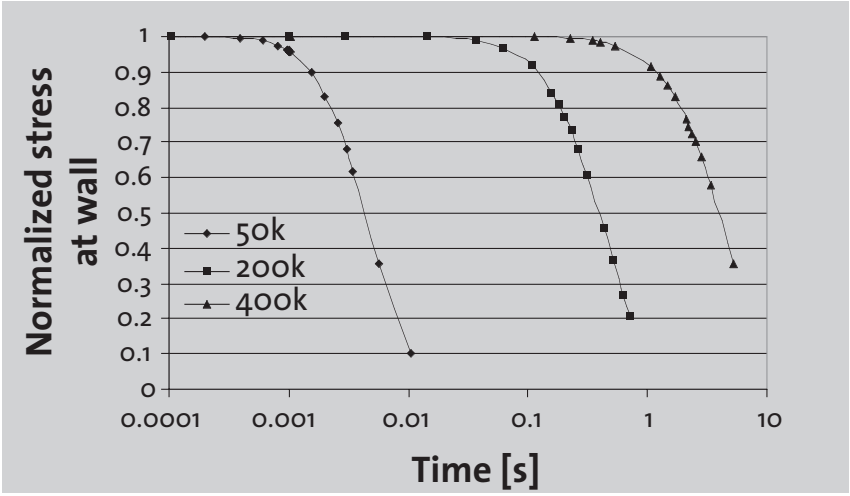

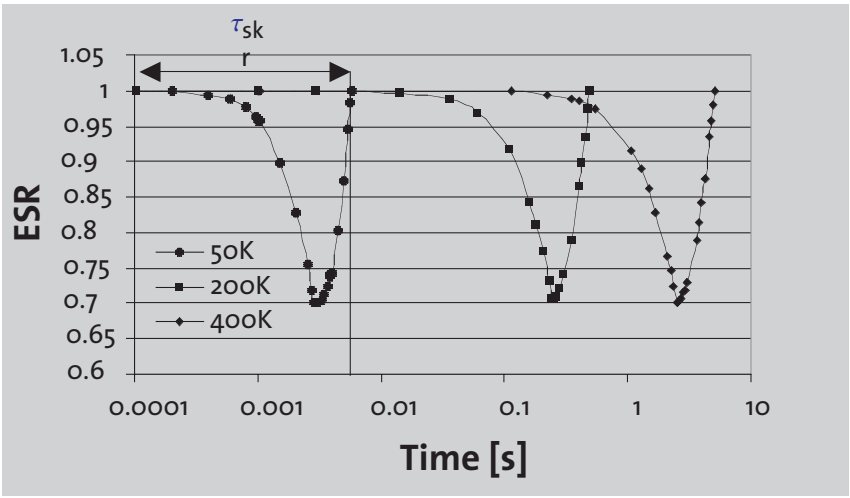

exit. The slip boundary condition is specified using the relation

$$F = -k \cdot v_s \tag{4}$$

where F is the force acting on the fluid at the wall, v_S is the slip velocity and k is a slip coefficient (the vectors F and v_S are obviously opposite in direction). The slip coefficient reflects the properties of the die surface. The higher the value of k, the more difficult for the polymer to slip. This leads to a higher force at the wall and a lower slip velocity.

In the simulations we modify the value of the k to control the stress level at the wall. The limitation of using this approach is the impossibility of simulating a stick boundary condition (k is finite and consequently there is always a finite slip velocity at the wall). As a consequence the stress fluctuation at the die exit causing sharkskin is simulated by modifying the k to reflect the oscillation of stress between its maximum value and 70% of this maximum. This is illustrated in Fig. 2b in contrast with Fig. 2a depicting the correct stick-slip mechanism of sharkskin formation. The presence of slip at the die exit reduces

Figure 6 (right above): Stress relaxation of three different molecular weight polybutadiene

Figure 7 (right below): Simulated stress fluctuations at the die exit for polybutadiene samples.

	Period		Amplitude
	Time [s]	Distance [mm]	[mm]
50K	0.0029	0.0668	0.0271
200K	0.228	0.0603	0.0266
400K	2.511	0.0517	0.0271

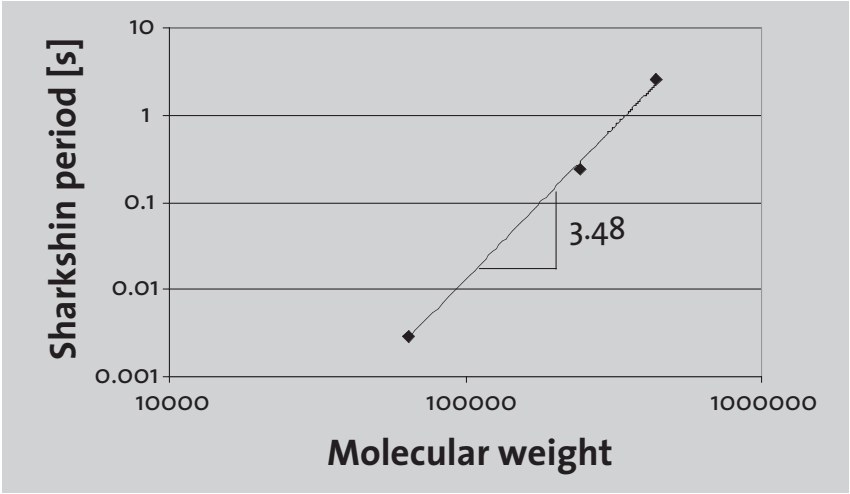

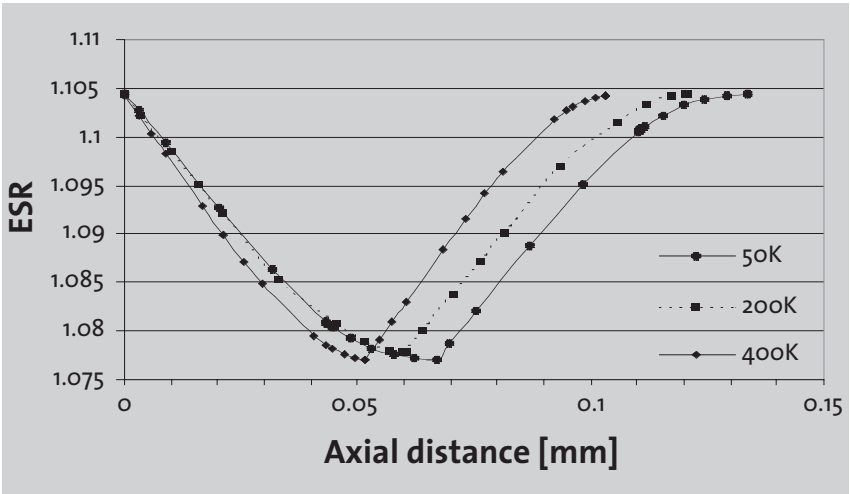

Table 1 (left above): Calculated values for the period and amplitude of simulated sharkskin.

Figure 8 (left middle): Sharkskin time period and molecular weight.

Figure 9 (left below): Simulated sharkskin results of polybutadiene samples.

the level of stress singularity and consequently affects the magnitude of the simulated extrudate swell ratio.

The equilibrium (steady-state) extrudate swell simulations were carried out at different levels of stress at the wall which were obtained using different values for the slip coefficient *k*. The different values for the slip coefficient were selected using a trial and error method designed to reproduce the stress relaxation/stress growth phenomena for the three materials investigated.

In each of the simulations we used no-slip boundary conditions at the die land, fully developed flow conditions at the inlet to the die, vanishing force at the outlet from the die and condition of zero normal velocity and zero tangential stress on the extrudate free surface. Details of the extrudate swell simulations can be found elsewhere [21].

6 RESULTS AND DISCUSSION

Results of stress relaxation ad stress oscillation for the three materials studied in this work are shown in Figs. 6 and 7, respectively. One can see clearly that the lower molecular weight polybutadiene relaxes much faster than the higher molecular weight materials. The sharkskin time period, τ_{shk}, was defined as the time for the stress to relax to 70% of its maximum level. The results are shown in Table 1. The 2.5s value obtained for the 400k polybutadiene at a wall stress level of 0.31 MPa comes very close to the experimental value of 2s obtained by Barone [14] for a similar material at 0.33 MPa. Moreover, our results for the sharkskin time period scale with the molecular weight at a power of 3.48, which comes close to the expected value of 3.4 (Fig. 8). Imbedded in this formalism is the notion that the polymer relaxation time scales linearly with the zero-shear viscosity.

The results of equilibrium extrudate swell simulations at different levels of stress at the wall can be plotted as a function of time using the stress relaxation/stress growth results for the different materials investigated. One can also easily convert the time axis to a distance axis by using the average velocity of the extrudate at the die exit. In Figure 9 we plot these results. It is interesting to observe that in spite of the large differences in sharkskin time period for the three materials investigated, the actual pictures of sharkskin look similar. This is not surprising since on an axial distance plot, periodicity is more a reflection of the level of stress applied which is kept constant for all three materials. The amplitude of sharkskin is also relatively constant for the three materials, reflecting the similarity in polydispersity for these samples. This result is similar to the one obtained in previous studies [21, 22]. The rather small differences in sharkskin distance period still suggest a shorter distance for the higher molecular weight material. This is in accordance with experimental data, which indicate more severe sharkskin development for higher molecular weight materials [22]. Again, at similar amplitude of sharkskin, the material with a shorter axial distance period will appear more severely distorted.

A comparison of the numerical results in Fig. 9 and experimental data (for instance results in Fig. 4 of reference [3]) show qualitative resemblance. The main problem is reproducing accurately the sharkskin amplitude mainly due to the limitations in depicting stress singularities, problems associated with the constitutive model employed in the simulations, limitation in mesh design refinement over a certain limit. In spite of these limitations, the qualitative agreement between simulation results and experimental data is good.

7 CONCLUSIONS

We simulated the sharkskin phenomenon based on a stick-slip mechanism. Simulation results were obtained using a superposition of stress relaxation/stress growth and a periodic change in extrudate swell governed by the die exit stress level. We first simulated the stress relaxation at the die wall upon cessation of flow in a circular die. This information was then used to simulate the extrudate swell at different levels of die exit stress. The die exit stress level was modified by way of a special slip region and a slip coefficient.

The simulated sharkskin time periods were found to be in good agreement with experimental data. Moreover, the sharkskin time period scales with the molecular weight at a power of 3.48, which comes close to the expected value of 3.4. We found that the simulated appearances of sharkskin are similar for all three molecular weight samples. The rather small differences in sharkskin distance periods mark shorter periods for the higher molecular weight materials.

A comparison between simulated sharkskin and experiments show qualitative resemblance. The main problems preventing us from quantitatively reproducing the sharkskin amplitude are the model limitations in depicting stress singularity, limitations in mesh design refinement and the constitutive model employed. In spite of these limitations, the qualitative agreement between the simulation results and experimental data is good.

ACKNOWLEDGMENTS

Nattapong Nithi-Uthai gratefully acknowledges the support of the Royal Thai Government. Computing services from the Ohio Supercomputer Center are also acknowledged.

REFERENCES

[1] Molenaar J, Koopmans RJ: Modeling polymer melt-flow instabilities. J. Rheology 38 (1994) 99-109.

[2] Georgiou GC, Crochet MJ: Time-dependent compressible extrudate-swell problem with slip at the wall. J. Rheology 38 (1994) 1745-1755.

[3] Venet C, Vergnes B: Experimental Characterization of Sharkskin in Polyethylenes, J. Rheology 41 (1997) 873-892.

[4] Graham MD: The sharkskin instability of polymer melt flows. Chaos 9 (1999) 154-163.

[5] Denn MM: Extrusion instabilities and wall slip. Annu. Rev. Fluid Mech. 33 (2001) 265-297.

[6] Barone JR, Plucktaveesak N, Wang S-Q: Interfacial Molecular Instability Mechanism for Sharkskin Phenomenon in Capillary Extrusion of Linear Polyethylenes. J. Rheology 42 (1998) 813-832.

[7] Wang S-Q, Drda PA, Inn Y-W: Exploring molecular origins of sharkskin, partial slip, and slope change in flow curves of linear low density polyethylene. J. Rheology 40 (1996) 875-898.

[8] Yarin AL, Graham MD: A model for slip at polymer/solid interfaces. J. Rheology 42 (1998) 1491-1503.

[9] Lipscomb GG, Keunings R, Denn MM: Implications of boundary singularities in complex geometries. J. Non-Newtonian Fluid Mech. 24 (1987) 85-96.

[10] Mhetar V, Archer LA: Slip in Entangled Polymer Solutions. Macromolecules 31 (1998) 6639-6649.

[11] Ahmed R, Liang RF, Mackley MR: The experimental observation and numerical prediction of planar entry flow and die swell for molten polyethylenes. J. Non-Newtonian Fluid Mech. 59 (1995) 129-153.

[12] Ahmed R, Mackley MR: Experimental conterline planar extension of polyethylene melt flowing into a slit die. J. Non-Newtonian Fluid Mech. 56 (1995) 127-149.

[13] Venet C, Vergnes B: Stress distribution around capillary die exit: an interpretation of the onset of sharkskin defect. J. Non-Newtonian Fluid Mech. 93 (2000) 117-132.

[14] Barone J, Wang S-Q: Flow birefringence study of sharkskin and stress relaxation in polybutadiene melts. Rheol. Acta 38 (1999) 404-414.

[15] Barone J, Wang S-Q: Rheo-optical observations of sharkskin formation in slit-die extrusion. J. Rheology 45 (2001) 49-59.

[16] Wang S-Q, Drda P: Molecular instabilities in capillary flow of polymer melts: interfacial stick-slip transition, wall slip and extrudate distortion. Macomol. Chem. Phys. 198 (1997) 673-701.

[17] Wang S-Q: Letter to the Editor - The mystery of the mechanism of sharkskin. J. Rheology 43 (1999) 245-252.

[18] Jay P: The reduction of viscous extrusion stresses and extrudate swell computation using slippery exit surfaces. J. Non-Newtonian Fluid Mech 79 (1998) 599-617.
[19] Giesekus H: A Simple Constitutive Equation for Polymer Fluids Based on the Concept of Deformation-Dependent Tensorial Mobility. J. Non-Newtonian Fluid Mech 11 (1982) 69-109.
[20] Yao M, McKinley GH, Debbaut B: Extensional deformation, stress relaxation and necking failure of viscoelastic filaments. J. Non-Newtonian Fluid Mech 79 (1998) 469-501.
[21] Nithi-Uthai N, Manas-Zloczower I: Numerical studies of the effect of constitutive model parameters as reflecting polymer molecular structure on extrudate swell, Appl. Rheol. 12 (2002) 252-259.
[22] Yang X, Wang S-Q, Chai C: Extrudate swell behavior of polyethylenes: Capillary flow, Wall slip, Entry/exit effects and Low temperature anomalies. J. Rheology 42 (1998) 1075-1094.